A Method for Automatic Extraction of Parotid Lesions in CT Images with Feature-Based Segmentation and Active Contour

Tung-Ying Wu and Sheng-Fuu Lin
National Chiao Tung University, Department of Electrical Engineering, Hsinchu, Taiwan (ROC).
Industrial Technique Research Institute, Center of Measurement and Standard, Hsinchu, Taiwan (ROC).
Email: tonyingwu@itri.org.tw, sflin@mail.nctu.edu.tw

Pa-Chun Wang and Yong-Cheng Wang
Cathay General Hospital, Taipei, Taiwan (ROC)
Email: {pachunwang, edwardwg }@cgh.org.tw

***Abstract*—In this paper, we propose a method that can be used to automatically segment and delineate the suspected lesion regions of parotid glands for computer-aided diagnosis and treatment planning on clinical applications. Because the suspected lesions are unpredictable, it needs to be found by distinguishing the local features of soft tissues. The proposed method starts from image sub-band decomposition and the gathered coefficients are utilized to derived local feature descriptors. The pixels of soft tissue regions can de segmented based on the corresponding local features and the pathological regions can be localized. In order to improve the accuracy of segmentation, the active contour method is then involved based on the segmentation results as the initial conditions. The active contour method is more sensitive to the gradient variation such that the initial conditions based on prior segmentation can help converge to the weak boundaries between pathological tissues and normal tissues. In this paper, the effective method that can improve medical automation is described, and the results are compared with the contour directly found by clinical experts. As a result, the experiment of H&N CT images with parotid lesions shows that the accuracy can approach over 94%.**

***Index Terms*—parotid, computer-aided diagnosis, computer tomography, active contour**

I. Introduction

Image-based computer-aided diagnosis (CAD) has been vigorously developed in recent years, because of the development of medical imaging techniques including ultrasound, positron emission tomography (PET) and computer tomography (CT). These imaging methods are originally used to observe the anatomical structures or lesions insides bodies and the captured images are viewed by the clinical experts. For the purpose to scrutinize the anatomical structures, CT is one of the most used method because the cross-sectional anatomical details can be shown in a series of sliced images. However, because of the complexity of the anatomical structures, it requires trained-experts to carefully find out the targets in the enormous number of gathered data. Although the anatomical structures can be presented in images, high noise and low contrast are still difficulties for inspection with naked-eye. In order to improve the efficiency of diagnosis, CAD is mentioned to assist clinical experts to confirm the diagnosis and reduce tedious manual procedures, and image-based CAD is proposed to automatically analyze the image data and extract the regions of interest (ROIs) to provide information about diagnosis in clinics. In order to improve medical automation, automatic segmentation of CT images is an important issue, and besides to automatically localize the bones and normal organs, in recent years, to automatically extract the pathological regions is also highly discussed to help clinical experts to find out the suspected lesions.

In Taiwan, according to the statistical data from official Department of Health (DOH), the amount of cases of cancers occurring at head and neck doubles in the past decades [1].

Parotid glands are the main salivary glands anatomically locating at both sides of the neck just in front of the ears. In clinics, parotid glands are concerned because not only malignant parotid tumors account for a dominant number of cancer cases in H&N, but the enlargement of parotid glands may also be associated with various H&N diseases, including cancer metastasis [2]. Besides, more than half of salivary gland tumor occurs in the parotid glands, and about 75% are benign [3]-[5]. For the purpose to observe parotid glands and the pathologies, CT slices perpendicular to the elongation of the spine are still the method used the most in clinics. Not only for aiding diagnosis of the increasing number of pathology cases, but also for the requirement of the modern therapies like intensity-modulated radiotherapy (IMRT), radiation treatment planning is to minimize the dose on treatment to reduce the harmful radiation toxicity for fear of serious side effects. Manual

Manuscript received August 18, 2013; revised November 18, 2013
This work was approved by Cathay General Hospital and the Institute Review Board (IRB) number is CGH-P101033.

doi: 10.12720/ijsps.1.2.225-231

procedures are exhausting and time-consuming, and besides, as the progress of medical imaging techniques, the amount of data becomes larger and larger, so computer-aided methods are in demand to reduce the burden of manual process. However, image qualities of low contrast and weak boundaries make soft tissue segmentation of gland regions more difficult than segmentation of the organ and bone regions. Although there have been works proposed to semi-automatically extract the parotid glands, it still hard to localize the suspected lesion regions well. Therefore, in order to improve the performance of CAD on parotid diagnosis, the segmentation of soft tissues and suspected lesions are important issues. In this paper, we propose a method comprising region-based segmentation and contouring algorithm to extract the suspected lesion tissues in parotid glands. In Section II, methods in previous works used to segment organs in CT are mentioned, and the previous works about parotid extraction were also discussed. In Section III, the proposed method used in this work is introduced, and in Section IV, some experiment results are presented and discussed, and in Section V, some conclusion and feature works are mentioned.

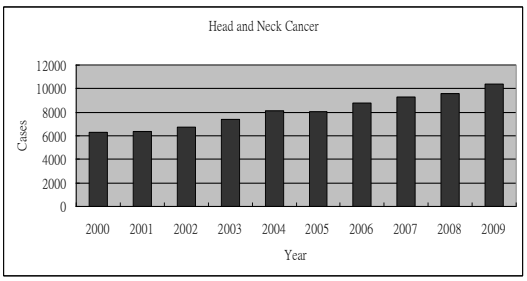

Figure 1. Number of case of head and neck cancer from 2000 to 2009 [1].

Figure 2. An H&N CT slice. The parotid glands are labeled (solid curves), and the pathological region is labeled with dotted curves.

II. Related Works

There have been various researches proposed to automatically or semi-automatically segment the organs or soft tissues in abdomen, brain and chest CT images. Because gray level is the most intuitive characteristic for region segmentation in CT images, methods based on gray level thresholding were discussed in many previous researches. However, unlike the bones or holes appearing in relatively high brightness or darkness in the CT images, it is hard to automatically decide the gray level ranges or thresholds to extract the target tissue regions. Traditional methods based on statistical analysis of gray level histogram to find a single threshold, like Otsu method [6], are not sufficient for segmenting soft tissues in CT images containing complex anatomical details and the regions without enough contrast. P. Campadelli *et al*. [7] proposed a method utilized regional gray level distribution to derive adaptive thresholds for segmenting livers filled with tissues in similar gray-level in abdominal CT images. In this work, livers occupying large area in images with tissues of uniform gray level were thought to result in peaks of histogram curve, so the gray level ranges corresponding to the tissue regions can be decided by determining the obvious peaks. In [8], Campadelli also extended this gray-level histogram-based method to segment more organs in abdomen CT images, including livers, kidneys and spleen, by determining the specific gray level ranges respectively. Moghe *et al*. [9] proposed a method to find the high thresholds and low thresholds by calculating the defined moment parameters of the histograms, and Yan and Wang [10] also proposed a gray-level based method to automatically segment the kidneys in CT images. Besides abdomen, in [11]-[19], methods based on gray level thresholding were also used to discriminate the tissue regions in CT images including lungs and mammography. However, simple gray level thresholding methods encountered difficulties because the thresholds were not so robust enough such that the variation of brightness and blurred boundaries of the targets may result in unsatisfying segmentation. Therefore, to improve the soft tissue segmentation, gray-level based methods in companion with local region clustering and morphological methods were proposed. Bae *et al.* [20] introduced a method comprising gray level thresholding, smoothing and pixel connectivity to find the regions filled with related pixels. Pohle and Toennies [21] also proposed the region-growing method to extract the soft tissues appearing with pixels of similar gray values. In [22], Kallergi *et al*. compared the performance of adaptive thresholding and region growing methods which were used in the segmentation of the mammography images. Methods based on measuring the relationship between pixels did not only rely on the determined thresholds, such that the regions filled with pixels with regional similarity could be found by clustering. In image-based CAD, to automatically find suspected regions related with lesions is an important issue to improve medical automation. In order to extract suspected lesion regions of the soft tissues, besides gray levels, the local features like textural characteristics and boundaries were also mentioned. In [23], adaptive thresholding method was used to segment the lesions in livers and in [24]; Mohanalin et al. used fuzzy-based method to segment the calcification of breast in mammography from the background. In [25]-[29], local features were adopted as characteristics to measure the

similarity of pixels for clustering to extract the lesion regions of breast, livers and lungs. These region-based extraction results were utilized to assist clinical experts to localize the lesions.

As to segmentation of parotid glands, besides region growing method mentioned in [30], active contour methods by means of atlas models as initial conditions were discussed in several previous works. Active contour models (ACMs) are efficient methods to generate closed boundaries of tissue regions, but effective initial conditions are required and highly affect the segmentation results. However, atlas-based models encountered difficulties on the deformation of soft tissues, so it needs preliminary evaluation to select appropriate models for fine extraction. In [31], Ramus and Malandian proposed an intensity-weighted majority vote to find the difference between the registered atlas images and the patient images. In [32], Yang et al. introduced principle component analysis (PCA) to determine the similarity of the atlas candidates with the patient images to choose an appropriate one as the initial condition for active contour iteration.

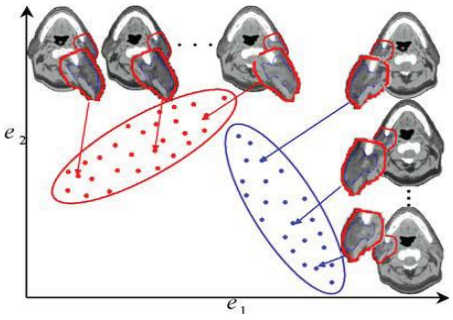

Figure 3. The demonstration of classification of atlas templates for parotid segmentation in [32].

In these works, the atlas models were built by collecting the data in clinics and modified with statistical regression. The approximate gland regions needed to be extracted manually for model selection and modification, and precise delineation were implemented by means of the modified models.

However, only normal glands without serious deformation can be built as models, but lesions are not expectable in their dimensions and may occur at unpredictable location. Therefore, it is hard to build applicable models as normal glands. To our knowledge, there are still no published reports about automatic delineation of the lesion regions in parotid glands in H&N CT images. Although region-based segmentation methods have less precision on segmentation, lesions can be automatically localized by the results. In previous researches about lesion segmentation with ACMs [33], [34], the initial conditions were set manually near the targets or geometrically with a circle or rectangle, but the contours were easily attracted by other strong boundaries during iterations. The boundaries between lesion regions and normal tissues are usually weak such that arbitrary initial contours are not sufficient.

III. Proposed Method

In order to delineate the suspected lesion regions of parotid glands without available templates, local image feature analysis method is proposed to segment soft tissues and localize the suspected pathological regions at first, and then the ACM is applied to delineate the suspected issue regions with higher accuracy. The segmentation results are modified as the initial conditions for ACM delineation. The following flow chart in Fig. 4 demonstrates the method proposed in this work, and the details of segmentation and delineation of parotid lesions are described in the following sections.

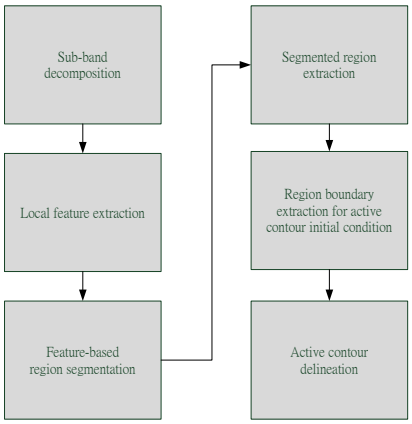

Figure 4. Schematic diagram of the proposed method.

A. Local Feature Extraction and Segmentation

In CT images, local features used the most are the gray values and their local statistical properties, but it is not sufficient enough for segmenting soft tissue regions. Hence, in this work, local variation reflecting the local texture characteristic is considered and the coefficients derived from *à trous* decomposition are utilized to derive the local characteristics [35]. The *à trous* decomposition can be considered as a method that can separate the high frequency component and low frequency component of an arbitrary signal into sub-bands. Therefore, there are two sub-bands, the approximate and detail sub-bands, generated after a one level decomposition. The approximate sub-band can be derived by convolving the original image with a low-pass filter, such as a Gaussian filter, and the detail sub-band can then be generated by subtracting the original image with the approximate sub-band image. Two-dimensional convolution can be implemented by convolving the filter with the image along both the row and column directions.

$$w_j(m,n) = c_{j-1}(m,n) - c_j(m,n) \quad (1)$$

where $w_j(m,n)$ means the detail coefficients at (m,n) in the sub-band, $c_j(m,n)$ means the approximation coefficients derived from convolving the input signal with a low pass filter at level j. $c_j(m,n)$ and $c_{j-1}(m,n)$ are approximation coefficients in successive scales at level j and level j-1. $c_0(m,n)$ means the original image. The decomposition of a level can be demonstrated as the figure below.

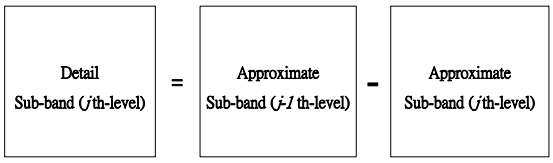

Figure 5. Demonstration of one-level sub-band decomposition.

It can be seen that the absolute values of detail coefficients are larger at the positions with higher variation such as the boundaries between soft tissues. Hence, the local variation can be measured by energy (*Eng*) and entropy (*Etp*) written as the equations below:

$$Eng = \frac{1}{N^2} \sum_{i,j \in mask} |W_{i,j}|^2 \tag{2}$$

$$Etp = -\frac{1}{N^2} \sum_{i,j \in mask} |W(i,j)|^2 \times \log(|W(i,j)|^2) \tag{3}$$

where $W_{i,j}$ means a coefficient at (i, j) inside a mask among a derived sub-band, and N is the number of elements inside the mask. By moving the mask among detail sub-bands, the two features corresponding to each pixel can be computed.

Segmentation can be implemented by clustering the local feature vectors composed of the gray value and the above local variation measures corresponding to each pixel. Mean shift is an effective method that can be used to cluster feature points with a preset bandwidth [36], [37]. The bandwidth is the parameter used to determine if a point belongs to a group or not. A Gaussian distribution function as (5) is usually adopted as a kernel function to evaluate the weight of a point in a group. The segmentation iteration proceeds by repeatedly computing the center of a group with points inside the bandwidth by the following equation.

$$x_c^{t+1} = \frac{\sum K(\|x_i - x_c^t\|) x_i}{\sum K(\|x_i - x_c^t\|)} \tag{4}$$

where K is the kernel function used to estimate the weight of a point, and x_c^t means the center at the tth iteration, c is a constant used to control the bandwidth.

$$K(\|x_i - x_c\|) = e^{-c\|x_i - x_c\|^2} \tag{5}$$

The iterative computation starts by randomly selecting center points, and terminates until the group centers vary within a small range. A segmentation procedure completes while all the feature points are assigned to their groups respectively. The feature-based segmentation method can connect pixels corresponding to soft tissues with similar local features into regions, and the suspected lesion regions can be localized after extracting the segmented regions from the results.

B. Suspected Lesion Extraction with Level Set ACM

After the soft tissue with similar features is approximately segmented into regions, the segmented regions can be extracted with morphological methods and contoured. The region boundaries can be utilized as the initial conditions for ACM to refine the tissue region segmentation. Because the derived region boundaries are near the real soft tissue boundaries, it has benefit to reduce the computation and prevent the contour from being attracted by other strong edges in the images. Mathematically, a contour C can be represented with the parametric vector equation

$$C(t) = (x(t), y(t)) \tag{6}$$

where t is the arc length parameter.

The energy function of a contour is consisted of external and internal energy, and can be written as the equation below:

$$E(C(t)) = \alpha \int_0^1 C'(t)^2 dt - \lambda \int_0^1 g(|\nabla I(C(t))|)^2 dt$$

$$= \int_0^1 E_{\text{int}}(C(t)) + E_{ext}(C(t)) dt \tag{7}$$

where $g(x)$ denote a stopping function used to move the contour toward the point with high gradient magnitude, can be set as the term below

$$g(x) = \frac{1}{\sqrt{1+x^2}} \tag{8}$$

The initial contour set by extracting the segmentation boundaries can evolve with obeying the equation

$$\frac{\partial C}{\partial t} = g(I)\kappa\vec{N} - (\nabla g(I) \cdot \vec{N})\vec{N} \tag{9}$$

where I means the gradient energy computed by

$$I(x(t), y(t)) = \sqrt{\left(\frac{\partial G(x(t), y(t))}{\partial x}\right)^2 + \left(\frac{\partial G(x(t), y(t))}{\partial y}\right)^2} \tag{10}$$

where $G(x,y)$ means the gray value at (x,y), κ represents the curvature and $\vec{N}$ is the unit inward normal.

Level set approach is the method used to evolve the contour in a two-dimensioned surface [38],[39], and the contour evolving equation (9) can be represented with level set approach as below,

$$\frac{\partial u}{\partial t} = g(I)\kappa|\nabla u| + \nabla g(I) \cdot \nabla u \tag{11}$$

where u is the signed distance map calculating the closest distance from a point in the map to the contour C and the points among C is consequently the zero level-set of u.

$$Dist(x,y) = \min_{(i,j) \in C_o} \left(\sqrt{(x-i)^2 + (y-j)^2}\right) \tag{12}$$

The initial distance map for active contour iteration is derived by computing the distance transform as (8) above of the boundary contour of the segmented regions.

IV. Experiment and Discussion

In this experiment, totally 80 images from 20 H&N CT sets with parotid single or double-sided pathology

selected by clinical experts are used in this experiment to evaluate the proposed method. These pathological images were collected from Cathay General Hospital and scanned by Phillip Brilliance 64 scanner with pixel spacing of the CT images $0.78 \times 0.78\text{mm}^2$. The segmentation results are compared with the results from clinical experts.

The following figures Fig. 6 and Fig. 7 demonstrate two examples of the experiment. The original CT images and the results at the steps including feature-based segmentation, region extraction and active contour delineation are shown as below.

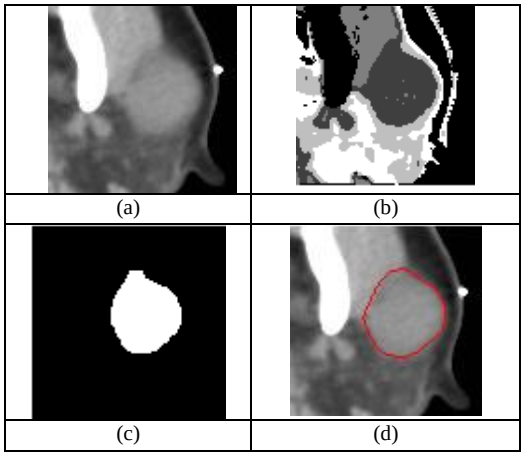

Figure 6. (a) Original image (b) Segmentation result (c) Extracted region (d) Active contour delineation result.

In Fig. 6(b), it can be seen that the soft tissue are segmented into regions, and each segmented region is labeled with different gray levels. However, the lesion region is similar with the muscle tissues and may not be perfectly separate. Morphological dilation and filling processes are used to break the connection between the similar tissues but it may also result in deformation of the lesion regions as shown in Fig. 6(c). Then, the extracted region is contoured as the initial condition for active contour computation, and the result is shown in red as in Fig. 6(d). The active contour converges to the points with higher gradient magnitude near the boundary of the extracted region in Fig. 6(c) and 4 iteration times are required in this example.

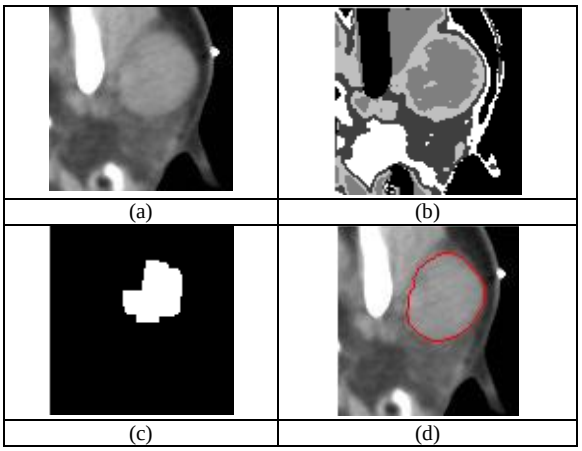

Figure 7. (a) Original image (b) segmentation result (c) extracted region (d) active contour delineation result.

In Fig. 7, the segmentation result does not effectively cover the lesion region and only the inner region with more uniform features is found. The extracted region also deforms a lot as shown in Fig. 7 (c). As a result, in Fig. 7(d) the active contour delineation can refine the result of segmentation and the iteration time is 9 at this experiment.

The accuracy of segmentation is evaluated by measuring the minimum distance between the results derived from the proposed method and the lesion region contoured by the clinical experts. The distance between two curves or contours can be derived by the following equation (13):

$$h(A,B) = \sum_{n_1 \in A} \min_{n_2 \in B}(A(n_1), B(n_2)) \tag{13}$$

where A and B are two contours and n_1 and n_2 mean the points belonging to A and B respectively.
The accuracy is defined as

$$acc = 1 - \frac{h(A,B)}{length(A)} \times 100\% \tag{14}$$

Each image is tested by the proposed method and the average accuracy of the segmentation over the 80 images can approaches over 94%.

V. Conclusion and Future Works

In this work, a method comprising region-based segmentation is proposed, and the experiments demonstrate the reliability of segmentation of the pathological regions of the tissues of the parotid glands. Localization of suspected regions can provide clinical experts to effectively focus on the pathology and automatic delineation can in advance provide information such as dimension and volume for further diagnosis or treatment planning. Future works include development of human interface to provide more apprehensive visual information on clinical application.

Acknowledgment

This research is approved by Cathay General Hospital and the Institute Review Board (IRB) number is CGH-P101033.

References

[1] Department of Health. ROC (Taiwan). [Online]. Available: https://cris.bhp.doh.gov.tw/
[2] B. Amirlak, H. Chim, E. H Chen, and D. W. Stepnick, Malignant Parotid Tumors. [Online]. Available: http://emedicine.medscape.com/article/1289616-overview
[3] The Merck manual for health care professional. Salivary Gland Tumors. [Online]. Available: http://www.merckmanuals.com/professional/ear_nose_and_throat_disorders/tumors_of_the_head_and_neck/salivary_gland_tumors.html
[4] Diagnosis and treatment of salivary gland cancer. [Online]. Available: http://cancer.stanford.edu/headneck/salivary.html
[5] G. L. Ellis, P. L. Auclair, and D. R. Gnepp, "Other malignant epithelial neoplasms," in *Surgical Pathology of the Salivary Glands*, W. Saunders Ed. 1991, pp. 455-488.

[6] N. Otsu, "A threshold selection method from gray-level histograms," in *Proc. IEEE. International Conference on System, Man, and Cybernetics*, vol. 9, 1979, pp. 62–66.
[7] P. Campadelli and E. Caseraghi, "Liver segmentation from computed tomography scans: A survey and a new algorithm," *Artificial Intelligence in Medicine*, vol. 45, no. 2-3, 2009.
[8] P. Campadelli, E. Caseraghi, S. Pratissoli, and G. Lombardi, "Automatic abdominal organ segmentation from CT images," *Electronic Letters on Computer Vision and Image Analysis*, vol. 8, no. 1, pp. 1-14, 2009.
[9] A. A. Moghe, J. Singhai, and S. C. Shrivastava, "Automatic threshold based liver lesion segmentation in abdominal 2D-CT images," *International Journal of Image Processing*, vol. 5, no. 2, 2011.
[10] G. Yan and B. Wang, "An automatic kidney segmentation from abdominal CT images," in *Proc. IEEE International Conference on Intelligent Computing and Intelligent Systems*, vol. 1, 2010.
[11] Q. Gao, S. J. Wang, D. Z. Zhao, and J. R. Liu, "Accurate lung segmentation for X-ray CT images," in *Proc. Third International Conference on Natural Computation*, 2007.
[12] B. Zheng, J. K. Leader III, G. S. Maitz, B. E. Chapman, C. R. Fuhrman, R. M. Rogers, F. C. Sciurba, A. Perez, P. Thompson, W. F. Good, and D. Gur, "A simple method for automated lung segmentation in x-ray CT images," in *Proc. SPIE*, vol. 5032, 2003, pp. 1455.
[13] A. Lauric and S. Frisken, "Soft segmentation of CT brain data," *Tufts University*, 2007.
[14] A. Padma and R. Sukanesh. "Automatic classification and segmentation of brain tumor in CT images using optimal dominant gray level run length texture features," *Int. J. Adv. Comp. Sci. Appl.*, vol. 2, no. 10, pp. 53-59, 2011.
[15] M. N. Hussien and M. I. Saripan, "Computed tomography soft tissue restoration using Wiener filter," in *Proc. 2010 IEEE Student Conference on Research and Development*. *IEEE*, 2010.
[16] P. Wei, J. Li, S. Zhao, D. Lu, and G. Chen, "A method of detection micro-calcifications in mammograms using wavelets and adaptive thresholds," *Bioinformatics and Biomedical Engineering, 2008. The 2nd International Conference on*. *IEEE*, 2008. (breast, wavelet, adaptive thresholding)
[17] K. Hu, X. Gao, and F. Li. "Detection of suspicious lesions by adaptive thresholding based on multiresolution analysis in mammograms," *IEEE Transactions on Instrumentation and Measurement*, vol. 60, no. 2, pp. 462-472, 2010.
[18] S. Hu, E. A. Hoffman, and J. M. Reinhardt, "Automatic lung segmentation for accurate quantitation of volumetric x-ray CT images," *IEEE Trans. Med. Imag.*, vol. 20, pp. 490-498, 2001.
[19] E. M. van Rikxoort, B. de Hoop, M. A. Viergever, M. Prokop, and B. V. Ginneken, "Automatic lung segmentation from thoracic CT scans using a hybrid approach with error detection," *Medical Physics*, vol. 36, no. 7, pp. 2934 – 2947, 2009.
[20] K. T. Bae, M. L. Giger, H. MacMahon, and K. Doi, "Automatic segmentation of liver structure in CT images," *Med. Phys.* vol. 20, no. 1, pp. 215-223, 1993.
[21] R. Pohle and K. D. Toennies, "Segmentation of medical images using adaptive region growing," *SPIE. Proc. Int. Soc. Opt. Eng.*, vol. 4322, pp. 1337-1346, 2001.
[22] M. Kallergi, K. Woods, L. P. Clarke, W. Qian, and R. A. Clark, "Image segmentation in digital mammography: Comparison of local thresholding and region growing algorithms," *Comput. Med. Imaging Graph*., vol. 16, no. 5, pp. 323-31, 1992.
[23] W. Seong, J. H. Kim, E. J. Kim, and J. W. Park, "Segmentation of abnormal liver using adaptive threshold in abdominal CT images," *IEEE. Nuclear Science Symposium Conference Record*, 2010.
[24] J. Mohanalin, P. K. Kalra, and N. Kumar, "Fuzzy-based micro calcification segmentation," in *Proc. International Conference on. Electrical and Computer Engineering IEEE*, 2008.
[25] W. Qian, L. P. Clarke, B. Zheng, M. Kallergi, and R. Clark, "Computer assisted diagnosis for digital mammography," *Engineering in Medicine and Biology Magazine IEEE*, vol. 14, no. 5, pp. 561-569, 1995.
[26] V. K. Gunturu and A. A. Sharma, "Contrast enhancement of mammographic images using wavelet transform," in *Proc. 3rd IEEE International Conference on Computer Science and Information Technology*. vol. 3, 2010.
[27] Y. Cao, X. Hao, X. Zhu, and S. Xia, "An adaptive region growing algorithm for breast masses in mammograms," *Frontiers of Electrical and Electronic Engineering in China*, vol. 5, no. 2, pp. 128-136, 2010.
[28] W. Seong, J. H. Kim, E. J. Kim, and J. W. Park, "Segmentation of abnormal liver using adaptive threshold in abdominal CT images," *IEEE. Nuclear Science Symposium Conference Record*, 2010.
[29] J. Wang, F. Li, and Q. Li, "Automated segmentation of lungs with severe interstitial lung disease in CT," *Med. Phy.*, vol. 36, no. 10, pp. 4592-4599, 2009.
[30] M. Mancas, B. Gosselin, and B. Macq. "Segmentation using a region-growing thresholding," *Electronic Imaging, International Society for Optics and Photonics*, pp. 388-398, 2005.
[31] L. Ramus and G. Malandain, "Multi-atlas based segmentation: Application to the head and neck region for radiotherapy planning," in *Proc. MICCAI Workshop Medical Image Analysis for the Clinic-A Grand Challenge*, 2010.
[32] J. Yang, Y. Zhang, L. Zhang, and L. Dong, "Automatic segmentation of parotids from CT scans using multiple atlases," *Medical Image Analysis for the Clinic: A Grand Challenge*, pp. 323-330, 2010.
[33] T. F. Chan and A. V. Luminita, "Active contour and segmentation models using geometric PDE's for medical imaging," in *Geometric Methods in Bio-Medical Image Processing*, Springer Berlin Heidelberg, 2002, pp. 63-75.
[34] Y. Wang, Z. X. Lin, J. G. Cao, and M. Q. Li, "Automatic MRI brain tumor segmentation system based on localizing active contour models," *Advanced Materials Research*, vol. 219, pp. 1342-1346, 2011.
[35] M. Holschneider, R. Kronland-Martinet, J. Morlet, and P. Tchamitchian, "A real-time algorithm for signal analysis with the help of the wavelet transform, in Wavelets," *Time-Frequency Methods and Phase Space*, pp. 289–297, 1989.
[36] Y. Cheng, "Mean shift, mode seeking, and clustering," *IEEE Transactions on Pattern Analysis and Machine Intelligence*, vol. 17, no. 8, pp. 790-799, 1995.
[37] D. Comaniciu and P. Meer, "Mean shift: A robust approach toward feature space analysis," *IEEE Transactions on Pattern Analysis and Machine Intelligence*, vol. 24, no. 5, pp. 603-619, May 2002.
[38] V. Caselles, R. Kimmel, and G. Sapiro, "Geodesic active contours," *International Journal of Computer Vision*, vol. 22, pp. 61-79, 1997.
[39] V. Caselles, F. Catte, T. Coll, and F. Dibos, "A geometric model for active contours," *Numerische Mathematik*, vol. 66, pp. 1-31. 1993.

Tung-Ying, Wu was born in Kaohsiung, Taiwan, in 1981. He received B.S degree in civil engineering in National Chiao Tung University in Hsinchu, Taiwan at 2003, and M.S degree in power machine engineering in National Tsing Hua University in Hsinchu, Taiwan at 2005. He is the candidate of Ph.D at institute of electric and control in National Chiao Tung University in Hsinchu, Taiwan. He works at Industrial Technique Research Institute at Hsinchu, Taiwan for software engineering. His current researches include image recognition, machine learning, image alignment, wavelet theory and application, medical image analysis and image-based computer-aided diagnosis.

Sheng-Fuu Lin was born in Tainan, ROC, in 1954. He received the B.S. and M.S. degrees in mathematics from National Taiwan Normal University in 1976 and 1979, respectively, the M.S. degree in computer science from the University of Maryland, College Park, in 1985, and the Ph.D. degree in electrical engineering from the University of Illinois, Champaign, in 1988. Since 1988, he has been on the faculty of the Department

of ElectricalEngineering at National Chiao Tung University, Hsinchu, Taiwan,where he is currently a Professor. His research interests include image processing, image recognition, image-based medical application including blood cell classification and computer-aided diagnosis, fuzzy theory, neural networks, automatic target recognition, intelligent system design and computer vision.

Pa-Chun Wang was born in 1964. He received the Medical Doctor (MD) degree from the China Medical University in 1990, and M.S. degree from the Harvard School of Public Health in 1995, and the EMBA degree from the National Taiwan University in 2013. Since 1990, he has been clinician and he is currently the head of the Department of Otolaryngology in the Cathay General Hospital in Taiwan, and he is also the professor in the School of Medicine, Fu Jen Catholic University, New Taipei, Taiwan. His research interests include otolaryngology, outcome research, healthcare quality and safety, health policy and management. He has been rewarded as an excellent clinical instructor, distinguish researchers several times since 2005, and the Certificate of Honor from the American Academy of Otolaryngology Head and Neck Surgery Foundation

Yong-Cheng Wang was born in 1960. He received the Medical Doctor (MD) degree from the Taipei medical university in 1987. Since 1987, he has been clinician and he is currently the head of the Department of Radiology in the Cathay general hospital in Taiwan, and he is also the clinical professor in the School of Medicine, Fu Jen Catholic University, New Taipei, Taiwan, and the Taipei Medical University, Taipei, Taiwan. His research interests include radiation-based diagnosis, ultrasound bone diagnosis and image-based computer-aided diagnosis. He was also the executive council member of Taiwan society of ultrasound in Medicine.